research papers

Experimental and theoretical characterization of the Zn—Zn bond in [Zn₂(η^5-C₅Me₅)₂]

Juan F. Van der Maelen,[a]*
Enrique Gutiérrez-Puebla,[b]
**Ángeles Monge,[b] Santiago
García-Granda,[a] Irene Resa,[c]
Ernesto Carmona,[c] María Teresa
Fernández-Díaz,[d] Garry J.
McIntyre,[d] Philip Pattison[e] and
Hans-Peter Weber[f]**

[a]Departamento Química Física y Analítica,
Facultad de Química, Avda. Julián Clavería 8,
University of Oviedo, E-33006 Oviedo, Spain,
[b]Instituto de Ciencia de Materiales, Consejo
Superior de Investigaciones Científicas, Sor
Juana Inés de la Cruz 3, E-28049 Madrid, Spain,
[c]Instituto de Investigaciones Químicas, Consejo
Superior de Investigaciones Científicas, Américo
Vespucio 49, E-41092 Sevilla, Spain, [d]Institut
Laue–Langevin, Av. des Martyrs BP 156, F-
38042 Grenoble CEDEX, France, [e]Swiss-
Norwegian Beam Lines, European Synchrotron
Radiation Facility, Jules Horowitz 6, BP 220,
F-38043 Grenoble CEDEX, France, and
[f]Laboratory of Crystallography, Swiss Federal
Institute of Technology, CH-1015 Lausanne,
Switzerland

Correspondence e-mail: fvu@uniovi.es

The existence and characterization of a bond between the Zn atoms in the recently synthesized complex [Zn₂(η^5-C₅Me₅)₂], as well as between Zn and ligand C atoms is firmly based on neutron diffraction and low-temperature X-ray synchrotron diffraction experiments. The multipolar analysis of the experimental electron density and its topological analysis by means of the 'Atoms in Molecules' (AIM) approach reveals details of the Zn—Zn bond, such as its open-shell inter-mediate character (the results are consistent with a typical metal–metal single bond), as well as many other topological properties of the compound. Experimental results are also compared with theoretical *ab initio* calculations of the DFT (density functional theory) and MP2 (Møller-Plesset pertur-bation theory) electron densities, giving a coherent view of the bonding in the complex. For instance, charges calculated from the AIM approach applied to the atomic basin of each Zn atom are, on average, +0.72 e from both the experimental and the theoretical electron density, showing a moderate charge transfer from the metal, confirmed by the calculated topological indexes.

1. Introduction

Recently, we reported (Resa *et al.*, 2004) the first stable molecular compound of zinc with a metal–metal bond, bis[1,2(η^5)-pentamethylcyclopentadienyl]dizinc(II)($Zn-Zn$), [Zn₂(η^5-C₅Me₅)₂] (1), which attracted great interest in the scientific community, and consequently three new species have been recently studied (Wang *et al.*, 2005; Zhu *et al.*, 2006; Grirrane *et al.*, 2007). These compounds have been char-acterized by a number of techniques (including NMR, IR and Raman spectroscopies, and conventional X-ray single-crystal diffraction) in order to demonstrate, among other things, the absence of any bridging H atom between the Zn atoms. The appearance of such an elusive metal–metal bond, in spite of the fact that organozinc compounds have been well known since the early days of organometallic chemistry, moved us to study synchrotron X-ray diffraction data, and also the theo-retical topological properties of the Zn—Zn bond.

Several theoretical calculations dedicated to (1) and related compounds have been published to date (Del Río *et al.*, 2005; Xie, Schaefer III & Jemmis, 2005; Xie, Schaefer III & King, 2005; Timoshkin & Schaefer III, 2005; Xie & Fang, 2005; Kress, 2005; Kang, 2005; Philpott & Kawazoe, 2006a,b; Pathak *et al.*, 2006). These studies, based on the molecular orbital (MO) approach, have found the minima in the potential energy surface of (1), with geometries that closely resemble the previously published experimental geometry. They have also shown that the Zn—Zn bond is comparable in stability to

Table 1
Experimental details.

	X-ray	Neutron
Crystal data		
Chemical formula	$C_{20}H_{30}Zn_2$	$C_{20}H_{30}Zn_2$
M_r	401.18	401.18
Cell setting, space group	Triclinic, $P\bar{1}$	Triclinic, $P\bar{1}$
Temperature (K)	100 (1)	170 (2)
a, b, c (Å)	6.9115 (6), 10.889 (1), 13.893 (1)	6.9329 (3), 10.8831 (5), 13.8384 (7)
α, β, γ (°)	109.91 (1), 101.551 (8), 93.905 (9)	109.777 (1), 101.603 (1), 94.201 (1)
V (Å^3)	952.6 (2)	951.09 (8)
Z	2	2
D_x (Mg m^{-3})	1.399	1.452
Radiation type	Synchrotron	White beam
μ (mm^{-1})	2.51	–
Crystal form, color	Plate, colorless	Prismatic, colorless
Crystal size (mm)	$0.70 \times 0.70 \times 0.05$	$2.0 \times 1.0 \times 0.3$
Data collection		
Diffractometer	CCD area detector	VIVALDI
Data collection method	φ and ω scans	Laue
Absorption correction	Multi-scan (based on symmetry-related measurements)	None
T_{min}	0.272	–
T_{max}	0.881	–
No. of measured, independent and observed reflections	57 003, 13 873, 12 354	8553, 1665, 985
Criterion for observed reflections	$I > 2\sigma(I)$	$I > 2\sigma(I)$
R_{int}	0.054	0.364
θ_{max} (°)	43.5	21.8
Refinement		
Refinement on	F	F^2
$R[F^2 > 2\sigma(F^2)]$, $wR(F^2)$, S	0.036, 0.040, 1.09	0.105, 0.264, 1.08
No. of reflections	11 249	1665
No. of parameters	782	469
H-atom treatment	Mixture of independent and constrained refinement	Mixture of independent and constrained refinement
Weighting scheme	$w = 1/[\sigma^2(F_o)]$	$w = 1/[\sigma^2(F_o^2) + (0.1322P)^2]$, where $P = (F_o^2 + 2F_c^2)/3$
$(\Delta/\sigma)_{max}$	0.047	0.032
$\Delta\rho_{max}$, $\Delta\rho_{min}$ (e Å^{-3})	0.59, −0.48	0.67, −0.60

Computer programs used: *CrysAlis CCD* and *CrysAlis RED* (Oxford Diffraction, 2004), *SORTAV* (Blessing, 1989), *SHELXL*97 (Sheldrick, 1997), *XD*2006 (Volkov *et al.*, 2006).

other metal–metal bonds, with dissociation energies calculated between 259.58 and 309.82 kJ mol^{-1} depending on the theoretical model used (Xie & Fang, 2005; Grirrane *et al.*, 2007). As far as we know, no studies related to the topological properties of the Zn—Zn bond, either from a theoretical or an experimental point of view, have been published so far, although some authors have mentioned the urgent need for such studies (Philpott & Kawazoe, 2006a). Our theoretical approach to this problem is based on the Quantum Theory of Atoms in Molecules (QTAM or AIM; Bader, 1990) and centred not only on the Zn—Zn bond, but also covering the Zn–ligand bonds. This treatment is complementary to the above-mentioned studies giving a fully coherent and more complete view of the bonding in (1) when combined with the MO calculations while, on the other hand, having the additional advantage of being equally applicable to both experimental and theoretical electron densities.

2. Experimental and computational details

2.1. Neutron diffraction experiment

A plate-like single crystal with maximum dimensions $2 \times 1 \times 0.3$ mm^3 was plucked from a pool of polyflorinether oil using a standard 1 mm diameter vanadium pin, and placed quickly in the pre-cooled helium-flow cryostat of the new Very-Intense Vertical-Axis Laue Diffractometer (*VIVALDI*) at the Institut Laue Langevin (ILL) in Grenoble (France) for the neutron diffraction experiment. *VIVALDI* uses the Laue diffraction technique on an unmonochromated thermal-neutron beam and with a large solid-angle (8 sterad) cylindrical image-plate detector (Wilkinson *et al.*, 2002) to increase the detected diffracted intensity by one-to-two orders of magnitude compared with a conventional monochromatic experiment. There were 17 Laue diffraction patterns, each accumulated over 2.5 h, collected at 170 K typically in 10° intervals during the rotation of the crystal perpendicular to the incident neutron beam. The patterns were indexed using the program *LAUEGEN* of the Daresbury Laboratory Laue Suite (Campbell, 1995; Campbell *et al.*, 1998) and the reflections integrated using the local program *ARGONNE_BOXES*, which uses a two-dimensional version of the $\sigma(I)/I$ algorithm (Wilkinson *et al.*, 1988). No correction for absorption was deemed necessary in view of the small crystal dimensions. The integrated reflections were normalized to a common incident wavelength, using a curve derived by comparing equivalent reflections and multiple observations, *via* the program *LAUENORM* (Campbell *et al.*, 1986). Reflections were observed with wavelengths between 0.85 and 3.56 Å, but only reflections with wavelengths less than 3.0 Å were accepted for scaling, as reflections at longer wavelength had too few equivalents to be able to determine the normalization curve with confidence. In all, 12 265 reflections were observed, of which 8553 were single well-resolved reflections with wavelengths between 0.85 and 3.0 Å, which yielded 1665 unique reflections, corresponding to 73.7% of the possible unique reflections for d spacings > 0.96 Å, the minimum d spacing observed. The conventional X-ray single-crystal parameters for non-H atoms (Resa *et al.*, 2004) were used as the initial model. The H atoms were all located from difference-Fourier maps. Refinements were carried out using

Table 2
Selected molecular geometry data (Å, °) for (1).

Bond distance or angle	Conventional X-ray†	Neutron diffraction‡	Multipole X-ray‡
Zn—Zn	2.305 (3)	2.292 (1)	2.3186 (3)
Zn—C§	2.268 (2)–2.306 (2)	2.272 (4)–2.326 (3)	2.2756 (12)–2.3132 (9)
Zn—Zn—C§	145.72 (6)–150.52 (6)	145.2 (4)–150.2 (4)	145.12 (6)–150.65 (4)

† Data from Resa *et al.* (2004). ‡ This work. § Lowest and highest values; individual values may be found in the supplementary material (Tables S1 and S2).
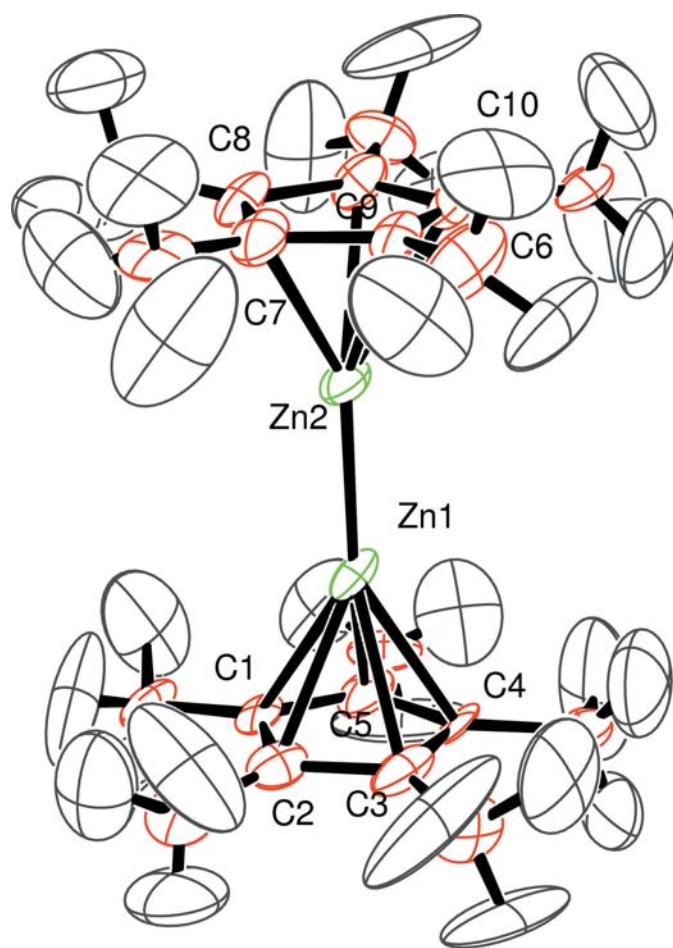

Figure 1
Displacement ellipsoid plot of (1) from the neutron diffraction experiment, drawn at the 80% probability level, showing the atomic labelling scheme (labels for H atoms are omitted for clarity).

*SHELXL*97 (Sheldrick, 1997) by full-matrix least-squares analysis with anisotropic displacement parameters for all atoms, including H atoms, with the latter considered as riding on their methyl groups. No disorder treatment was applied here to the methyl groups. Further details are given in Table 1 and the molecular geometry obtained is shown in Fig. 1. As may be clearly seen in Fig. 1, no bridging H atoms were found between the Zn atoms. This result was the main purpose of the neutron diffraction experiment, *i.e.* to eliminate the remote possibility of having missed bridging hydride ligands in the prior experimental studies, as certainly happened in the well

known proposed cobalt compound $[Co_2(\eta^5\text{-}C_5Me_5)_2]$, firstly reported as having a Co—Co bond but which, in fact, is a hydride (Kersten *et al.*, 1992). For the experimental charge-density study the results were obtained from the synchrotron X-ray experiment without the use of neutron data.

2.2. Synchrotron X-ray diffraction experiment

In order to obtain better data for the multipolar refinement than the data collected previously from conventional X-ray diffraction, a synchrotron diffraction experiment was performed. A laminar colorless single crystal of $0.70 \times 0.70 \times 0.05$ mm^3 was selected. Measurements were carried out at the BM01A (Swiss–Norwegian Beam Line) of the European Synchrotron Radiation Facility (ESRF) in Grenoble (France). Data collection was *via* a KUMA KM6-CH (equipped with a CCD detector) six-circle κ single-crystal diffractometer, utilized as a standard four-circle instrument. The data collection temperature, controlled by an Oxford cryostream cooling system, was 100 (1) K, and the wavelength of the radiation used was 0.71 Å.[1] The experimental strategy was as follows:

(i) a good diffracting crystal was selected (the crystal was mounted on the diffractometer and a couple of frames were observed prior to starting the complete data collection);

(ii) around 20 frames were then collected for indexing purposes;

(iii) a run of *ca* 2 h of data collection was then used to try and solve the structure;

(iv) finally the full dataset was collected.

In fact, three different datasets were collected at this stage: a high-angle dataset, using no filter, was collected first; then a low-angle dataset was collected using a 50 μm Cu filter; finally a very low-angle data collection was performed with a 100 μm Cu filter. A total of 57 003 reflections were measured $[(\sin\theta/\lambda)_{max} = 1.08$ Å$^{-1}]$, covering 90.3% of all possible reflections from $\theta = 2.01°$ to θ_{max}. Data reduction was then applied using the *SORTAV* program (Blessing, 1989), giving a total of 13 873 unique reflections ($R_{int} = 0.054$), and an absorption correction was also applied using *SADABS* (Sheldrick, 2003; Blessing, 1995). Solution and standard (spherical atoms) refinement were made using the *WinGX* program package (Farrugia, 2005). Some disorder in the methyl groups was observed during the refinement and therefore some were split into two components in order to prevent them from being non-positive definite using the usual constraints (Van der Maelen Uría & Sheldrick, 1996; Van der Maelen Uría, 1999). Further details for this experiment are given in Table 1.[2] A selection of the molecular geometry data, compared with the results from neutron diffraction, is shown

[1] In our proposal for the experiment, different experimental conditions were asked for: a wavelength of 0.5 Å and a temperature of 10 K, but only a more standard set-up was made available.
[2] Supplementary data for this paper are available from the IUCr electronic archives (Reference: BS5050). Services for accessing these data are described at the back of the journal.

in Table 2. All in all, due mainly to a greater redundancy of the data collected, a better precision than in the conventional X-ray diffraction experiment was achieved, as reflected in the lower standard deviations (see §3 for more detailed comments).

2.3. Multipole refinement

The multipole refinement was carried out by means of the program *XD*2006 (Volkov *et al.*, 2006), which uses the Hansen–Coppens formalism for the aspherical atomic density expansion (Hansen & Coppens, 1978). Several models were tried, but the best results were obtained with a treatment that proceeded as follows. Hexadecapole representation was used for the Zn and C atoms, while the H atoms were treated as oriented dipoles, with their coordinates fixed, during the early stages of the multipole refinement process, at the positions found in the spherical-atom refinement. An average distance of 1.0495 Å, obtained from the neutron diffraction experiment, was used later as a constraint for all the C—H bond distances. Radial parts for core, spherical-valence and deformation-valence densities were all constructed using relativistic Dirac–Fock atomic wavefunctions expanded over Slater-type basis sets for the Zn atoms (Su & Coppens, 1998), while for C and H atoms the radial parts of the deformation valence densities were single-ζ Slater-type functions. Further constraints were used to keep the refined parameters of all the H atoms within each methyl group equal. Radial scaling parameters for the spherical and deformation parts of the valence density (κ and κ_l'; $l = 0$–4) were independently refined for both Zn atoms, while for the C atoms only κ and κ_0' were independently refined, using the constraint $\kappa_l' = \kappa_0'$ ($l = 1$–4) for the other scaling parameters. For the H atoms all these parameters were left fixed to their default values. In addition, occupation factors for the two components of the disordered methyl groups that were split during the spherical atom refinement were left fixed at their earlier values (P_{val} parameters). A total of 782 parameters were refined against the 11 249 'observed' reflections [$F > 3\sigma(F)$] included in the refinement ($N_{ref}/N_{par} = 14.4$). The final conventional R factor over F was 0.036 for the 'observed' reflections and 0.043 for the whole set of unique reflections. Refinement values given in Table 1 are for what we consider to be the 'best' experimental model (BE model), in the sense that it has the best final statistical indexes (R, S, $\Delta\rho_{max,min}$, difference Fourier map, convergence criteria *etc.*), but we also used other multipole models in the topological calculations in order to further check their accuracy against topological indexes (see below).

2.4. Experimental and theoretical topological calculations

The *XDPROP* module of the program *XD*2006 (Volkov *et al.*, 2006) was used to study the topological properties of the experimental electron density by means of the AIM approach (Bader, 1990; Coppens, 1997). Both local (location of critical points and bond-path analyses, among others) and integral properties (atomic charges, volumes, dipole moments *etc.*) were calculated. Usually the calculations were carried out

using the default values given by the program for the different control parameters; however, for the integral properties several integration parameters had to be tested and modified in order to increase the accuracy of the results. The beta-sphere radii of the atoms were taken, for the integrations, as the distance between the atom nucleus and its closest bond-critical point (b.c.p.). Starting from the 'best' experimental model obtained in the multipolar refinement, as defined above, the procedure followed was able to find all the b.c.p.s in the molecule, whereas for the other models several b.c.p.s were either missing or located at odd positions (*e.g.* between the H atoms of different methyl groups). Accordingly, only the BE model was used to obtain the computationally lengthy integral properties.

On the other hand, both molecular geometries obtained from neutron and X-ray diffraction experiments were used for the theoretical electronic structure calculations performed using the *GAUSSIAN*03 program package (Frisch *et al.*, 2004). The electronic structure calculations were performed on the experimental geometries using both DFT and *ab initio* perturbation theory methods. The following methods were used: the hybrids B3LYP, B3P86 and B3PW91 Becke's three-parameter exchange functional (Becke, 1993) with the non-local Lee-Yang-Parr (Lee *et al.*, 1988), Perdew (Perdew, 1986) and Perdew-Wang (Perdew *et al.*, 1996) correlation functionals, respectively, and the Vosko–Wilk–Nusair local correlation functional (Vosko *et al.*, 1980), together with the Møller–Plesset MP2 and MP3 methods were tried. All-electron standard basis sets 6-31G(d), 6-31G(d,p) and 6-311G(d,p) have been used for all atoms as is usual for other calculations of organometallic compounds (Van der Maelen Uría *et al.*, 2003, 2005). The ground-state electronic wavefunctions obtained were then used for further calculations on the topology of the theoretical electron density, including both local and integral properties, performed with the aid of the program *AIM*2000 (Biegler-König & Schönbohm, 2002). The accuracy of the integrated properties was finally set at 1.0×10^{-4} from the Laplacian of the integrated electron density, whereas for the local properties the accuracy was much greater (1.0×10^{-10} from the gradient of the electron density at the b.c.p.s). Some theoretical models (a combination of molecular geometry, method and basis set) were able to find all the b.c.p.s found from the 'best' experimental (BE) model, but the best results, in the sense that theoretical local properties were close to the experimental ones, were obtained using the MP2/6-311G(d,p) model with the neutron diffraction geometry (BT model). In fact, some calculations made on the X-ray diffraction geometry were even unable to find the Zn—Zn b.c.p. Consequently, integral properties were then calculated using only the BT model, which we call the 'best' theoretical model.

3. Results and discussion

Neutron diffraction experiments carried out at the ILL (see §2) provided us both with experimental evidence of the absence of bridging H atoms between the Zn atoms in (1), and

with the nuclear coordinates to be used in the theoretical electronic structure calculations, as explained earlier. The molecular geometry, shown in Fig. 1, does not differ much from the previous results (Resa *et al.*, 2004), giving the typical sandwich structure already proposed. In Table 2 some relevant bond distances and angles obtained from the neutron diffraction data and from the X-ray synchrotron diffraction data are compared with previously available values from conventional X-ray diffraction. As may be seen from the table, the Zn—Zn distance obtained from the neutron diffraction experiment is shorter than the distances found from both X-ray data, whereas the Zn—C distances are only slightly longer and the main bond angles are almost the same. The neutron Zn—Zn distance in (1) is even shorter than the same distance in the bulk metal, so there could be an extra repulsion from the core electrons of the two metal atoms that would push them away from the intermetallic region, therefore giving an X-ray distance larger than the neutron value. Published theoretical calculations for the optimized geometry of (1) show Zn—Zn distances over a wide range, varying from 2.287 to 2.339 Å, depending on the theoretical model used (Grirrane *et al.*, 2007; Kress, 2005; Xie & Fang, 2005). On the other hand, conventional X-ray experimental data obtained for two recently synthesized compounds, $Zn_2[\{(2,6-^iPr_2C_6H_3)-N(Me)C\}_2CH]_2$ (Wang *et al.*, 2005) and $Zn_2\{C_6H_3-2,6-(C_6H_3-2,6-^iPr_2)_2\}_2$ (Zhu *et al.*, 2006), gave Zn—Zn distances of 2.3586 (7) and 2.3591 (9) Å, respectively.

In order to obtain good quality electron densities suitable for an experimental topological analysis (Coppens, 1997; Koritsanszky & Coppens, 2001; Coppens *et al.*, 2005) we
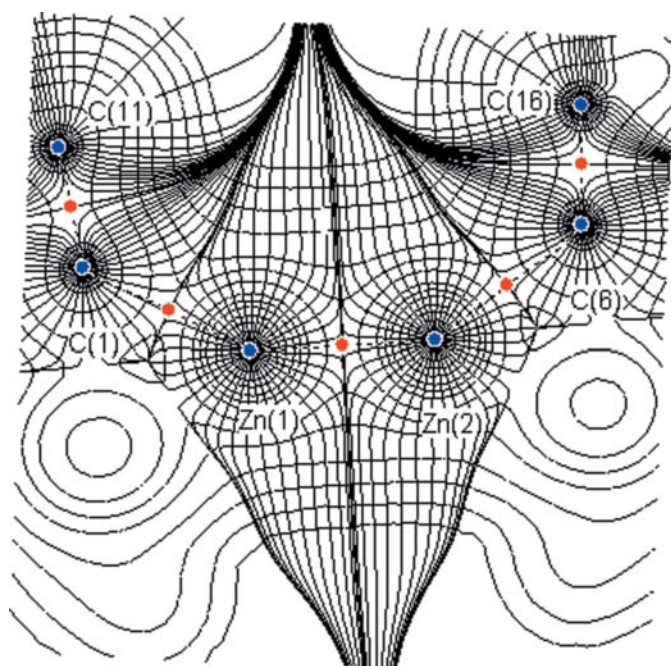
carried out a multipolar analysis of the experimental electron density obtained from the synchrotron X-ray data described in §2, followed by the application of the AIM approach (Bader, 1990). This analysis gave a consistent view of a fully connected molecule, including the complete set of one b.c.p. between the Zn atoms, 10 b.c.p.s between Zn and C atoms, 20 b.c.p.s for the C—C bonds and 30 b.c.p.s for the C—H bonds, together with the 12 ring critical points (r.c.p.) and two cage critical points (c.c.p.). In Fig. 2 a gradient trajectory map for (1) is shown, where the critical point and the bond path (b.p.) between the Zn atoms are clearly seen. Also shown are the b.c.p.s and b.p.s found between each of the Zn atoms, and the C-Me group in the ligand ring located in the plane of the plot. Owing to the (nearly) cylindrical symmetry of the molecule, the image in Fig. 2 may be rotated around the Zn—Zn axis to obtain a complete picture of the electron-density gradient field. In fact, very similar plots are found if different planes are selected. Furthermore, our theoretical calculations made at the *ab initio* level show results that closely resemble experimental calculations. For instance, charges calculated from the AIM approach applied to the atomic basin of each Zn atom are, on average, +0.720 e from the experimental electron density and

Figure 2
Gradient trajectories mapped on a total density plot (contour levels at 0.1 e Å^{-3}) for the Zn2—Zn1—C1 plane of (1). B.c.p.s (red circles) and b.p.s (dashed lines) are also shown.
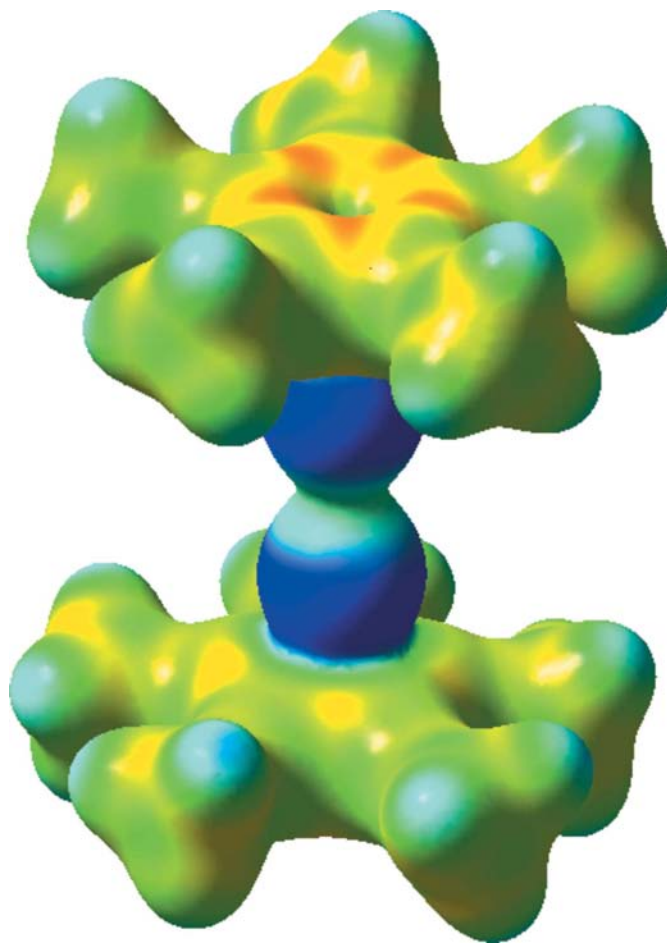

Figure 3
Three-dimensional representation of the molecular electrostatic potential mapped on an electron density isosurface. Color codes from +0.567 (dark blue) to −0.002 e Å^{-1} (dark red). Density contour value: 0.27 e Å^{-3}.

Table 3
Selected experimental (first row) and theoretical [second row, MP2/6-3111G(d,p) level] topological parameters for (1).

d_{A-B}: bond path length; ρ_b: electron density at the b.c.p.; $\nabla^2\rho_b$: Laplacian of the electron density at the b.c.p.; H_b/ρ_b: total energy density ratio at the b.c.p. (see text); G_b/ρ_b: kinetic energy density ratio at the b.c.p.; $\delta(A-B)$: delocalization index (see text); $\oint_{A\cap B}\rho$: integrated electron density (see text).

Bond distance	d_{A-B} (Å)	ρ_b (e Å^{-3})	$\nabla^2\rho_b$ (e Å^{-5})	H_b/ρ_b (h e^{-1})	G_b/ρ_b (h e^{-1})	$\delta(A-B)$	$\oint_{A\cap B}\rho$ (e Å^{-1})
Zn—Zn	2.3206 (3)	0.348 (3)	1.824 (17)				
	2.1657	0.426	1.622	−0.361	0.627	0.919	1.252
Zn—C†	2.2642 (12)	0.398 (8)	1.952 (20)				
	2.1699	0.332	3.922	−0.160	1.118	0.225	0.254

† Average values.

+0.725 e from the theoretical electron density. These values are slightly lower than the formal charge of +1 e empirically postulated for the Zn atoms in (1) and, compared with other theoretical values obtained from MO approaches (Resa *et al.*, 2004; Kang, 2005; Kress, 2005; Grirrane *et al.*, 2007), suggest the existence of a certain amount of charge transfer from the ligands (see below). Accordingly, average experimental and theoretical charges for the ten C atoms of the two Cp* rings are −0.39 and −0.27 e, respectively. Fig. 3 shows the experimental electrostatic potential mapped on an electron density isosurface.

In Table 3 a summary of the topological properties calculated from both experimental and theoretical electron densities is shown. As clearly seen in the table, the experimental value for the Zn—Zn bond length calculated from the bond path (see Fig. 2) matches almost perfectly the X-ray synchrotron interatomic distance (Table 2), hence showing no bending in the bond path. Although the theoretical value reflects a slight bending, giving a difference of only 0.15 Å between the theoretical bond-path length and the experimental interatomic distance, it is fair to conclude that this is a nearly perfect σ bond, a result which is confirmed by the extremely low ellipticity calculated for this bond (0.001). This result is in line with previous results, based on NBO and similar MO analyses (Kress, 2005; Grirrane *et al.*, 2007), which show that the Zn—Zn bond is mainly formed by interaction of the 4s metal orbitals, although with small contributions from p_σ and d_σ orbitals (Philpott & Kawazoe, 2006a). Current bond classifications based on the atomic valence shell for molecules involving heavy atoms make use of both local (at the b.c.p.) and integral (over the atomic basin) properties (Macchi *et al.*, 2002; Macchi & Sironi, 2003; Gervasio *et al.*, 2004, 2005; Gatti, 2005). Among the former, the electron density (ρ_b), the Laplacian of the electron density ($\nabla^2\rho_b$), the total energy density ratio (H_b/ρ_b) and the kinetic-energy density ratio (G_b/ρ_b), with $H(\mathbf{r}) = G(\mathbf{r}) + V(\mathbf{r})$ and $\frac{1}{4}\nabla^2\rho(\mathbf{r}) = 2G(\mathbf{r}) + V(\mathbf{r})$ [$V(\mathbf{r})$ is the potential energy density], are by far the most common. From the values in Table 3 it is clear that the Zn—Zn bond in (1) is a typical open-shell metal–metal bond (*e.g.* Co—Co, Macchi *et al.*, 2002; Macchi & Sironi, 2003; or Ru—Ru, Stash *et al.*, 2005), which differs from a pure covalent bond (such as C—C in ethane). This result is confirmed by the integral properties listed in Table 3, *i.e.* the delocalization index, δ(Zn—Zn), and the electron density integrated over the whole Zn—Zn interatomic surface, $\oint_{Zn\cap Zn}\rho(\mathbf{r})$. The former is indeed

nearly equal to the formal bond order of 1.0, showing that there is just one electron pair shared by the two atoms, while the latter has a value comparable in magnitude to that of pure covalent bonds (2.16 for the C—C bond in ethane; Gatti, 2005, and references therein), despite the fact that ρ_b is one order of magnitude lower for (1).

Some topological properties for the Zn—Cp* interactions are also listed in Table 3. There is more literature on the topological properties of metal–ligand bonds than for metal–metal bonds, but they are mainly centred on metal–CO interactions (Pillet *et al.*, 2003; Stash *et al.*, 2005; Farrugia *et al.*, 2006). It is not unusual to find just one bond path between a metal and a π-bound ligand similar to Cp* (*e.g.* the Zr–indenyl interactions; Stash *et al.*, 2005). As mentioned above, a most remarkable feature of the topological analysis for the Zn—C interactions in (1) is that some, although not all, of the models tried, both experimental and theoretical, provided the ten b.c.p.s and bond paths between the Zn and C atoms, a pair of which is shown in Fig. 2. Therefore, in this case it is fair to conclude that we are concerned here with real bonds, not just 'interactions', in the sense that real bond paths have been found between Zn and C atoms. The topological parameters also reflect this fact; for instance, the value of the delocalization index listed in Table 3 for each of the five Zn—C bonds is large enough to confirm the above assertion and, in addition, suggests than just one electron pair is shared between a Zn atom and its bonded Cp* ring. The values for the other topological magnitudes shown in the table are very similar to those found in other metal—C bonds, notably some Zr—C(indenyl) (Stash *et al.*, 2005) and Zr—C(imine) (Pillet *et al.*, 2003) bonds. According to the classification of Macchi and Sironi (Macchi & Sironi, 2003), they are not purely ionic bonds but they may be labelled as donor–acceptor bonds, with a moderate charge transfer revealed by the relatively modest value of $\oint_{Zn\cap C}\rho(\mathbf{r})$. Moreover, since the average experimental bond path length for the Zn—C bond in (1) differs only slightly from the average experimental interatomic distance (0.03 Å), it can be said that these are nearly straight bonds and therefore there is a nearly pure transfer of approximately one electron from each metal atom to its ligand. Finally, from the clearly large values found for the experimental (3.21) and theoretical (4.20) ellipticities, it must be concluded that the Zn—C bonds in (1) have a definite π character, in agreement with previous theoretical studies based on MO theory (Xie & Fang, 2005; Philpott & Kawazoe, 2006a,b).

research papers

4. Conclusions

In summary, the existence and characterization of a bond between the Zn atoms in the complex $[Zn_2(\eta^5\text{-}C_5Me_5)_2]$, as well as between the Zn and the Cp^* C atoms, have been firmly based on neutron diffraction and low-temperature X-ray synchrotron diffraction experiments, together with the multipolar analysis of the experimental electron density and the topological analysis *via* the AIM approach of both the experimental and the theoretical electron density. Further studies on this complex based on maps of the Laplacian of the electron density, as well as other properties, including the topological analysis of the ligands themselves, are in progress in our laboratory.

References

Bader, R. F. W. (1990). *Atoms in Molecules: A Quantum Theory*. Oxford: Clarendon Press.

Becke, A. D. (1993). *J. Chem. Phys.* **98**, 5648–5652.

Biegler-König, F. & Schönbohm, J. (2002). *J. Comput. Chem.* **23**, 1489–1494.

Blessing, R. H. (1989). *J. Appl. Cryst.* **22**, 396–397.

Blessing, R. H. (1995). *Acta Cryst.* A**51**, 33–38.

Campbell, J. W. (1995). *J. Appl. Cryst.* **28**, 228–236.

Campbell, J. W., Habash, J., Helliwell, J. R. & Moffat, K. (1986). *Inf. Q. Protein Crystallogr.* **18**, 23–31.

Campbell, J. W., Hao, Q., Harding, M. M., Nguti, N. D. & Wilkinson, C. (1998). *J. Appl. Cryst.* **31**, 23–31.

Coppens, P. (1997). *X-ray Densities and Chemical Bonding*. Oxford Science Publications.

Coppens, P., Iversen, B. & Larsen, F. K. (2005). *Coord. Chem. Rev.* **249**, 179–195.

Del Río, D., Galindo, A., Resa, I. & Carmona, E. (2005). *Angew. Chem. Int. Ed.* **44**, 1244–1247.

Farrugia, L. J. (2005). *WinGX Program System*, Version 1.70.01. University of Glasgow, Scotland.

Farrugia, L. J., Frampton, C. S., Howard, J. A. K., Mallinson, P. R., Peacock, R. D., Smith, G. T. & Stewart, B. (2006). *Acta Cryst.* B**62**, 236–244.

Frisch, M. J. *et al.* (2004). *GAUSSIAN*03, Revision C.02. Gaussian Inc., Pittsburgh, PA, USA.

Gatti, C. (2005). *Z. Kristallogr.* **220**, 399–457.

Gervasio, G., Bianchi, R. & Marabello, D. (2004). *Chem. Phys. Lett.* **387**, 481–484.

Gervasio, G., Bianchi, R. & Marabello, D. (2005). *Chem. Phys. Lett.* **407**, 18–22.

Grirrane, A., Resa, I., Rodríguez, A., Carmona, E., Álvarez, E., Gutiérrez-Puebla, E., Monge, A., Galindo, A., del Río, D. & Andersen, R. (2007). *J. Am. Chem. Soc.* **129**, 693–703.

Hansen, N. K. & Coppens, P. (1978). *Acta Cryst.* A**34**, 909–921.

Kang, H. S. (2005). *J. Phys. Chem. A*, **109**, 4342–4351.

Kersten, J. L., Rheingold, A. L., Theopold, K. H., Casey, Ch. P., Widenhoefer, R. A. & Hop, C. E. C. A. (1992). *Angew. Chem. Int. Ed.* **31**, 1341–1343.

Koritsanszky, T. S. & Coppens, P. (2001). *Chem. Rev.* **101**, 1583–1627.

Kress, J. W. (2005). *J. Phys. Chem. A*, **109**, 7757–7763.

Lee, C., Yang, W. & Parr, R. G. (1988). *Phys. Rev. B*, **37**, 785–789.

Macchi, P., Garlaschelli, L. & Sironi, A. (2002). *J. Am. Chem. Soc.* **124**, 14173–14184.

Macchi, P. & Sironi, A. (2003). *Coord. Chem. Rev.* **238**, 383–412.

Oxford Diffraction (2004). *CrysAlis*. Oxford Diffraction, Abingdon, Oxfordshire, UK.

Pathak, B., Pandian, S., Hosemane, N. & Jemmis, E. D. (2006). *J. Am. Chem. Soc.* **128**, 10915–10922.

Perdew, J. P. (1986). *Phys. Rev. B*, **33**, 8822–8824.

Perdew, J. P., Burke, K. & Wang, Y. (1996). *Phys. Rev. B*, **54**, 16533–16539.

Philpott, M. R. & Kawazoe, Y. (2006*a*). *Theochem.* **773**, 43–52.

Philpott, M. R. & Kawazoe, Y. (2006*b*). *Chem. Phys.* **327**, 283–290.

Pillet, S., Wu, G., Kulsomphob, V., Harvey, B. G., Ernst, R. D. & Coppens, P. (2003). *J. Am. Chem. Soc.* **125**, 1937–1949.

Resa, I., Carmona, E., Gutiérrez-Puebla, E. & Monge, A. (2004). *Science*, **305**, 1136–1138.

Sheldrick, G. M. (1997). *SHELXL*97. University of Göttingen, Germany.

Sheldrick, G. M. (2003). *SADABS*. University of Göttingen, Germany.

Stash, A. I., Tanaka, K., Shiozawa, K., Makino, H. & Tsirelson, V. G. (2005). *Acta Cryst.* B**61**, 418–428.

Su, Z. & Coppens, P. (1998). *Acta Cryst.* A**54**, 646–652.

Timoshkin, A. & Schaefer III, H. F. (2005). *Organometallics*, **24**, 3343–3345.

Van der Maelen Uría, J. F. (1999). *Crystallogr. Rev.* **7**, 125–180.

Van der Maelen Uría, J. F., Ruiz, J. & García-Granda, S. (2003). *J. Appl. Cryst.* **36**, 1050–1055.

Van der Maelen Uría, J. F., Ruiz, J. & García-Granda, S. (2005). *J. Theor. Comput. Chem.* **4**, 823–832.

Van der Maelen Uría, J. F. & Sheldrick, G. M. (1996). *Anal. Quim. Int. Ed.* **92**, 7–12.

Volkov, A., Macchi, P., Farrugia, L. J., Gatti, C., Mallison, P. R., Richter, T. & Koritsanszky, T. (2006). *XD*2006. University of New York at Buffalo, USA.

Vosko, S. H., Wilk, L. & Nusair, M. (1980). *Can. J. Phys.* **58**, 1200–1211.

Wang, Y., Quillian, B., Wei, P., Wang, H., Yang, X. J., Xie, Y., King, R. B., Scheleyer, P. R., Schaefer III, H. F. & Robinson, G. H. (2005). *J. Am. Chem. Soc.* **127**, 11944–11945.

Wilkinson, C., Cowan, J. A., Myles, D. A. A., Cipriani, F. & McIntyre, G. J. (2002). *Neutron News*, **13**, 37–41.

Wilkinson, C., Khamis, H. W., Stansfield, R. F. D. & McIntyre, G. J. (1988). *J. Appl. Cryst.* **21**, 471–478.

Xie, Y., Schaefer III, H. F. & Jemmis, E. D. (2005). *Chem. Phys. Lett.* **402**, 414–421.

Xie, Y., Schaefer III, H. F. & King, R. B. (2005). *J. Am. Chem. Soc.* **127**, 2818–2819.

Xie, Z.-Z. & Fang, W.-H. (2005). *Chem. Phys. Lett.* **404**, 212–216.

Zhu, Z., Wright, R. J., Olmstead, M. M., Rivard, E., Brynda, M. & Power, P. P. (2006). *Angew. Chem. Int. Ed.* **45**, 5807–5810.